Modelling Stability Improvement In Kazakhstan's Power System By Using Battery Energy Storage

Ansar Berdygozhin
Electronic and Electrical Engineering
the University of Strathclyde
Glasgow, the UK
ansar.berdygozhin@strath.ac.uk

Dauren Akhmetbayev
Electrical Engineering and Electronic Engineering
Kazakh AgroTechnical University
Nur-Sultan, Kazakhstan
axmetbaev46@mail.ru

David Campos-Gaona
Electronic and Electrical Engineering
the University of Strathclyde
Glasgow, the UK
d.campos-gaona@strath.ac.uk

***Abstract*—Kazakhstan is going to increase share of RES up to 10% until 2030 and up to 50% until 2050. The current share of RES is 3% and BESSs are not used. This paper analyzes the simplified national power grid and the ability of BESS participation in frequency regulation in accident loss of generation on one of the stations. The results show that BESS only is not enough to keep frequency in desirable restrictions.**

Keywords—BESS, stability, Kazakhstan, power systems, synthetic inertia

I. INTRODUCTION

Kazakhstan, adopted in 2013 the concept for Transition of the Republic to Green Economy [1]. Which states that the share of renewable energy resources (RES) in the power system of the country should be 3% by 2020, 10% by 2030 and 50% by 2050 [1]. The first goal of the concept was achieved in 2020, as reported by the ministry of the energy of Republic of Kazakhstan [2]. However, the current share of RES, as well as the prospects of further RES penetration in the power grid is a matter of concern to the Kazakhstan electric grid operating company (KEGOC) because of intermittent behaviour of RES [3]. This is mainly because in order to provide uninterrupted power, KEGOC obligates conventional power plants to reserve some amount of power by which the intermittence can be compensated, which in turn is not cost effective. Some countries smooth the RESs power output is by having manoeuvrable power sources such as hydro power plants which have the capability to synchronize with the power grid and provide the necessary power in a fast manner without the need of conventional thermal power plants. However, since Kazakhstan has lack of such power plants the government aims to increase them in the near future to cope with the increasing penetration of RES. Thus, in the current situation thermal power plants keep some generator units in hot and spinning reserve which increases production outlays.

One way of enhancing stability in power system and its flexibility to allow more RES penetration is the usage of battery energy storage systems (BESS). Reference [4] shows that BESS power capacity for frequency regulation depends on wind power penetration level and rate of change of power of conventional generators. Authors in [5] conclude that BESS has advantage over STATCOM for stability purposes since it can provide both active and reactive power during a transient event.

Given the documented advantages of BESS for stability improvements and flexibility of power networks, this paper revises the application of BESS in the Kazakhstan power network and evaluates its performance using simulations. To do this, this paper uses an accurate representation of the Kazakhstan power network suitable for electromechanical simulations (i.e. phasor representation). Proper controllers in the *dq0* frame and in DC for the BESS are designed to provide a synthetic inertia response from the energy storage asset, and the impact of different levels of energy storage power and control variables are evaluated for a loss-of-generation scenario.

This paper is organized as follows: Section II presents the model of the Kazakhstan Power System. Section III presents the design of BEES controllers for synthetic inertia provision and its incorporation into a phasor model environment. Section III presents a set of simulation cases that verify the performance of the BESS and the behaviour of the grid frequency for different levels of energy storage size and a set of simulation cases with different low pass filter (LPF) time constants. Section IV presents simulation results and V presents conclusion.

II. MODELLING OF KAZAKHSTAN POWER SYSTEM

Fig. 1 represents simplified Kazakhstan's power system which consists of 500 kV transmission power lines and main thermal power plants. The electric power transmission networks can be found in [6], where can be seen that Kazakhstan's power system is a part of synchronous zone (unified/integrated power system, UPS/IPS). Wind and solar power plants were eliminated to simplify the model. The main thermal power stations are located in the North because of coal sources there, so the South Kazakhstan has energy deficit. Thus, power flows through 500 kV overhead power lines from the north to the south, which is more than 900 km. All power lines, in the model, have the same reactance and capacitance per unit length, which are L=0.8737 mH/km and C=13.33 nF/km, and were modelled by standard π model. The surge impedance loading (SIL) of power lines can be calculate by (1), where V is rated voltage, and L, C were determined earlier.

$$SIL = \frac{V^2}{\sqrt{L/C}} = \frac{(500\cdot10^3)^2}{\sqrt{(8.7\cdot10^{(-4)})/(13.3\cdot10^{(-9)})}} = 976.5\,MW \quad (1)$$

So, power flow from power stations through the lines was set to be close to SIL value of the line. The parameters of the different elements used in the model are provided in the Appendix. The transition power flow is replaced by Load 5 (Ld5). G1, G2, G3 from Fig. 1 represent conventional thermal power stations, whereas G4 represents aggregated hydro power stations which are in the East Kazakhstan and are close each other. All generator parameters were aggregated following the consideration presented in [7], [8]. The parameters of transformers have the same impedance values except rated power and can be found in the Appendix as well. G5 is a power station which is considered to be built and does not exist at the moment.

978-1-6654-4407-1/21/$31.00 Â©2021 IEEE

This is a peer reviewed, accepted author manuscript of the following research paper: Berdygozhin, A., Akhmetbayev, D., & Campos-Gaona, D. (2021). Modelling stability improvement in Kazakhstan's power system by using battery energy storage. In 2021 56th International Universities Power Engineering Conference (pp. 1-5). IEEE. https://doi.org/10.1109/UPEC50034.2021.9548180

The BESS was placed to be close to power loads. The model was built in Matlab&Simulink and was simulated using phasors. [9] recommends to use the phasor solution method to model electromechanical oscillations for power system as it employs all differential equations related to stator and rotor electromechanical transients, but in the meantime saves computational resources when compared with time-based simulations.

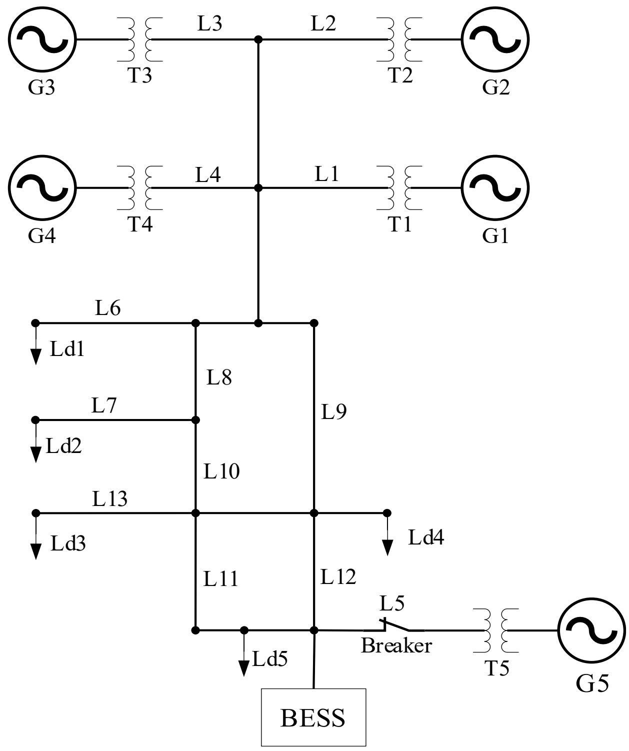

Fig. 1. The simplified power system of Kazakhstan.
(connections between nodes without marks are the same nodes)

III. Modelling of BESS for Phasor Simulations

In order to comprise the BESS model which includes power electronics into the phasor model, the battery was replaced by its mathematical model configured as voltage source to satisfy the phasor solution method, as seen in Fig. 2. Where input is current calculated from the measured power and the output is the voltage of the BESS.

The battery grid converter was replaced by the controlled current sources, as seen in Fig. 3, where i_a(t) and i_b(t) are control signals. These control signals are generated according to Fig. 4 block scheme. Where, V_{abc}^{g} and I_{abc}^{g} are measured voltage and current of the grid, v_{d1} and v_{q1} are the *d* and *q* components of the AC grid voltage, θ is the angle of the grid voltage, i_{d1} and i_{q1} are the *d* and *q* components of the measured current, i_d^* and i_q^* are the reference *d* and *q* components of current, v_{d2} and v_{q2} are the *d* and *q* components of the average inverter voltage, L_l

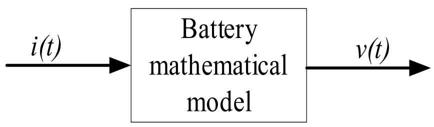

Fig. 2. BESS representation in solution method [10].

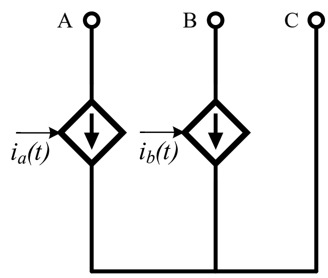

Fig. 3. Converter representation in phasors solution method.

and R_l represent values of link between inverter and AC grid and are equal to 0.92437 mH and 1.5 mΩ respectively, ω is angular frequency of the grid, i_d and i_q are the *d* and *q* components of the $i_a(t)$ and $i_b(t)$ control signals and are calculated by (3).

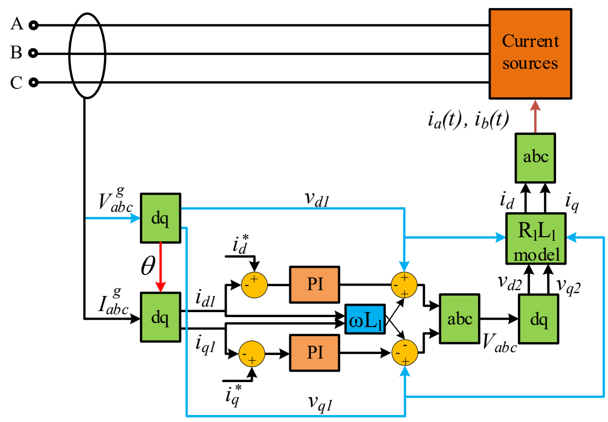

Fig. 4. BESS control block scheme.

The R_lL_l model block in Fig. 4 is the mathematical representation of a resistor + inductor interface between the converter and the AC grid. The dynamics of the current circulating between this interface is given as

$$v_{d1} - v_{d2} = i_d R_l - i_q L_l \omega + L_l \frac{di_d}{dt}$$
$$v_{q1} - v_{q2} = i_q R_l + i_d L_l \omega + L_l \frac{di_q}{dt} \qquad (2)$$

and particularly its frequency domain form

$$i_d = \frac{\omega}{L_l s}\left(v_{d1} - v_{d2} - i_d R_l + i_q L_l\right)$$
$$i_q = \frac{\omega}{L_l s}\left(v_{q1} - v_{q2} - i_q R_l - i_d L_l\right) \qquad (3)$$

The *dq* transformation of the measured 3-phase voltage and current phasors is shown in Fig. 5. Where first, the positive sequence voltage and currents are obtained following (4), where, a is an operator equal to a phase shift of 120°, V_1 and I_1 are positive sequence voltage and current (4), V_a, V_b, V_c and I_a, I_b, I_c are the *abc* voltages and currents measured at the connection point. Next V_1 and I_1 are converted to polar representation, where the angle of positive sequence voltage V_1 is θ, which is used to calculate the phase angle of I_1 against V_1. The last stage of the block diagram converts the polar representation of V_1 and I_1 to cartesian values, which are then used to obtain v_{d1}, v_{q1}. To align v_{d1} with x-axis (i.e. the *d* axis) the angle of V_1 was set to 0.

$$V_1 = \frac{1}{3}\left(V_a + aV_b + a^2V_c\right)$$
$$I_1 = \frac{1}{3}\left(I_a + aI_b + a^2I_c\right) \quad (4)$$

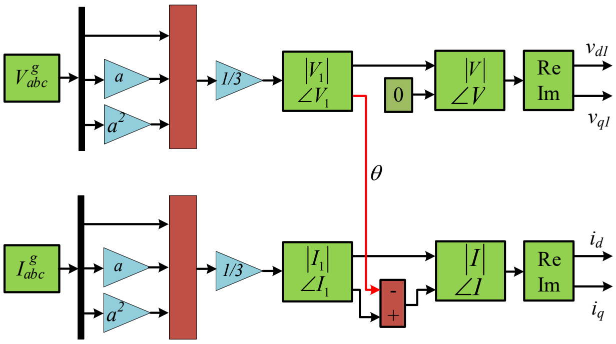

Fig. 5. *dq* transformation in phasors solution method.

The BESS control the *d* current using power electronics to produce an active power output. The reference i_d^* current is computed by (5), Fig. 6, as a difference between reference active power P^* and measured active power P_m.

$$P^* - P_m = \frac{3}{2} v_{d1} i_d^* \quad (5)$$

The G_1 gain and the integrator block are added to slow down response dynamics due to physical restrictions of BESS response.

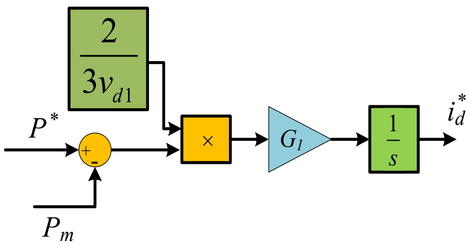

Fig. 6. Computing reference i_d current inside the BESS control structure.

The active power reference P^* is computed by using block scheme on Fig. 7. The input signals are the reference frequency f^*, 50 Hz or 60 Hz, and measured average frequency f_{av} which is calculated as a sum of angular speeds of rotors ω in p.u. multiplied by f^* and divided by number of generators, such method helps to avoid using frequency measurement block which can have severe numerical errors. DZ – is a dead zone filter which enables to avoid unnecessary battery triggering according to grid code, and increases lifespan of it as well. For Kazakhstan, it is ±10 mHz for primary frequency regulators under [11] 5.3.2. LPF – stands for low pass filter which is used to cutoff frequencies above setpoint value. DD – is a discrete derivative which implements battery triggering to rate of change of frequency (ROCOF). G_2 – is a gain which is a simple proportional regulator and the last block represents saturation.

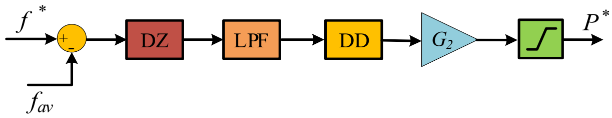

Fig. 7. Computing reference active power *P* inside the BESS control structure.

IV. Simulation Results

The simulation was computed for three rated power of BESS: 500 MW, 250 MW, 100 MW, and without BESS, case 1, and with different low pass filter time constants for 250 MW power BESS, case 2.

A. Case 1: BESS with different power rates

The results are shown on Fig. 8. At 5th second power station G5 with power line L5 are disconnected by the breaker. Due to loss of generation power balance changes which leads to the grid frequency decreasing. The lowest frequency dip, as it can be expected, is without BESS and then it goes up in proportion to BESS power. So, the minimum of the blue curve is 49.9256 Hz and the minimum of the purple curve which corresponds to 500 MW BESS is 49.9339 Hz. The difference is only 8.3 mHz. At the same time, 500 MW BESS can be too expensive. Thus, in a such severe disturbance, as loss of power station which consists

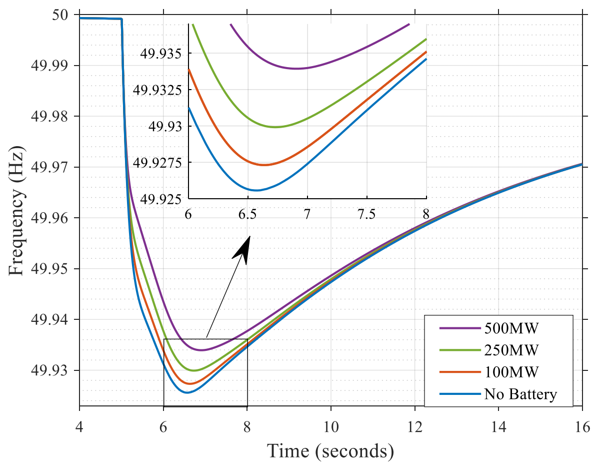

Fig. 8. The average frequency for different rated power BESS.

approximately 12.6% of the generated power, BESS is not enough to keep frequency in the needed ±20 mHz deviation.

B. Case 2: low pass filter with different time constants

The mathematical representation of a simple LPF, shown in Fig. 7, in is given in the frequency domain by (6), where τ is time constant. To determine the influence of the cutoff frequency on ROCOF different τ time constants where used: 0.1 ms, 0.1/3 ms, 0.1/6 ms, 0.1/9 ms. The Bode plot and cutoff frequencies of which are shown in Fig. 9.

$$LPF = \frac{1}{1+\tau s} \quad (6)$$

The cutoff frequencies can be found analytically by (7), where ω_c is angular cutoff frequency, or graphically by locating intersections of curves and a line drawn from -3 dB on Bode magnitude plot, the dashed line in Fig. 9.

$$\omega_c = \frac{1}{\tau} \quad (7)$$

With the selected time constants, the cutoff frequencies turn to be 100 rad/s, 300 rad/s, 600 rad/s, 900 rad/s which equal to 15.91 Hz, 47.75 Hz, 95.49 Hz, and 143.24 Hz, respectively. The result of simulations using synthetic inertia provision with different low pass filters is shown in Fig. 10, where it can be seen that the average frequency nadir and overall frequency response is very similar for LPF with the selected time constants. It can be concluded that

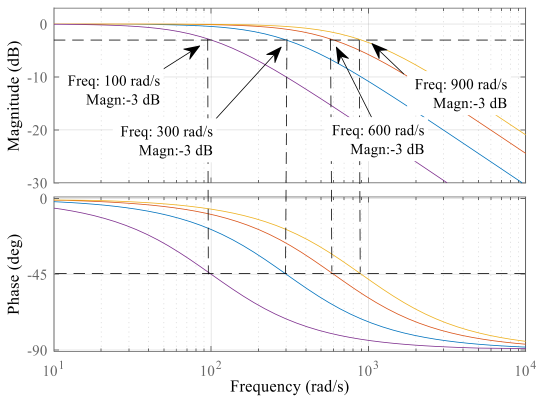

Fig. 9. Bode diagram of used LPF. Cutoff frequencies are the intersections of the curves and the dashed line.

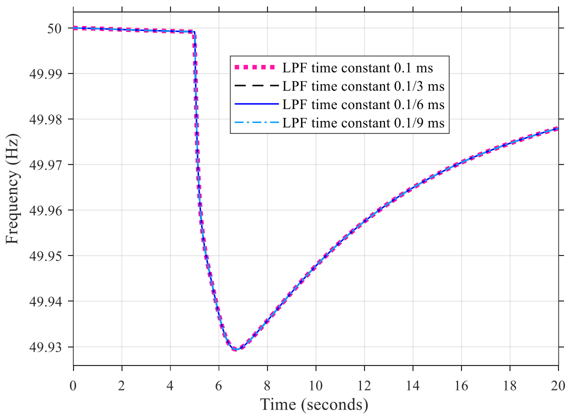

Fig. 10. The average frequency for different time constant, τ , LPF.

due to the slow rate of change of frequency, it is enough to have relatively low bandwidth (low cutoff frequency) for the filters. This is desirable since it increases the immunity of noise and the robustness of the deployment. However, further investigation is necessary to assess the impact of the delay of the low pass filters to the provision of the synthetic inertia response from the batteries under noisy environments and delays in frequency measurements.

V. Conclusion

This study provided a simulation environment where the impact of energy storage response is evaluated in a realistic representation of the Kazakhstan network. The developed model uses phasor simulation which enable the analysis of electromechanical transients in larger power networks without extensive computation requirements. A phasor battery energy storage model, along with its control systems was designed and included into the phasor model. The simulation results demonstrated the correct performance of the BESS model and the developed power network.

This study found that synthetic inertia provided by BESS with rated power 100 MW, 250 MW, 500 MW is not enough to keep the average frequency in needed ±20 mHz limit according to grid code during loss of generation on station G5. This evidences that even highly sensitive energy storage response in not enough to meet the grid codes. Although the amount of energy storage penetration in the power network could be increased, this will not be a realistic scenario given the price of energy storage and converters needed to supply sufficient frequency response. This calls into attention the use of other frequency containment mechanisms, such as synthetic inertia from wind power, or some sort of fast power supply by new HVDC-Based interconnectors. Future studies will analyse the implication of having these mechanisms applied to the Kazakhstan network.

VI. Appendix

Table I

Loads	Power (MW)
Ld1	900
Ld2	200
Ld3	200
Ld4	100
Ld5	1800

Table II

Lines	Length (km)
L1	0
L2	40
L3	120
L4	330
L5	0
L6	294
L7	0
L8	273
L9	550
L10	256
L11	381
L12	384
L13	410

TABLE III

Power stations	The number of generators	Rated power, kVA	Xd (pu)	Xd' (pu)	Xd" (pu)	Xq (pu)	Xq' (pu)	Xq" (pu)	Xl (pu)	Td' (ms)	Td" (µs)	Tq' (ms)	Tq" (ms)	Stator resistance (pu·10^{-3})	Inertia, H (S)
G1	7	588	2.31	0.318	0.222	2.31	0.318	0.264	0.268	1.01	32	1.01	32	2.1	8.09
G2	2	588	2.31	0.318	0.222	2.31	0.318	0.264	0.268	1.01	32	1.01	32	2.1	8.09
G3	7	352	2.195	0.3	0.195	2.195	0.3	0.195	0.17	1.14	25	1.14	25	2.1	4.47
G4	5	352	2.195	0.3	0.195	2.195	0.3	0.195	0.17	1.14	25	1.14	25	2.1	4.47
G5	4	352	2.195	0.3	0.195	2.195	0.3	0.195	0.17	1.14	25	1.14	25	2.1	4.47

ACKNOWLEDGMENT

The authors gratefully acknowledge the chief dispatcher of the National dispatching centre of KEGOC Dr. Beckzhan Mukatov for the discussions.

REFERENCES

[1] "Concept on Transition towards Green Economy until 2050." https://policy.asiapacificenergy.org/node/133#:~:text=KAZAKHSTAN%3A%20Concept%20on%20Transition%20towards%20Green%20Economy%20until%202050&text=The%20Concept%20aims%20to%20increase,the%20energy%20security%20of%20Kazakhstan.

[2] "The share of renewable energy in Kazakhstan will reach 6 by 2025%." Ministry of Energy of the Republic of Kazakhstan. https://www.gov.kz/memleket/entities/energo/press/news/details/dolya-vie-v-kazahstane-k-2025-godu-dostignet-6?lang=en.

[3] Z. Mominbayev, "Forecasting of generation by RES," *QazaqGreen,* vol. 1, no. 1, p. 4, 01.04.2021 2021. [Online]. Available: https://spaq.kz/images/QazaqGreen_1_2021_EN.pdf.

[4] C. Liang, P. Wang, X. Han, W. Qin, Y. Jia, and T. Yuan, "Battery Energy Storage Selection Based on a Novel Intermittent Wind Speed Model for Improving Power System Dynamic Reliability," *IEEE Transactions on Smart Grid,* vol. 9, no. 6, pp. 6084-6094, 2018, doi: 10.1109/TSG.2017.2703578.

[5] U. Datta, A. Kalam, and J. Shi, "Battery Energy Storage System to Stabilize Transient Voltage and Frequency and Enhance Power Export Capability," *IEEE Transactions on Power Systems,* vol. 34, no. 3, pp. 1845-1857, 2019, doi: 10.1109/TPWRS.2018.2879608.

[6] M. Karatayev and M. L. Clarke, "A review of current energy systems and green energy potential in Kazakhstan," *Renewable and Sustainable Energy Reviews,* Review vol. 55, pp. 491-504, 2016, doi: 10.1016/j.rser.2015.10.078.

[7] R. Singh, M. Elizondo, and S. Lu, "A review of dynamic generator reduction methods for transient stability studies," in *2011 IEEE Power and Energy Society General Meeting*, 24-28 July 2011 2011, pp. 1-8, doi: 10.1109/PES.2011.6039791.

[8] A. J. Germond and R. Podmore, "Dynamic Aggregation of Generating Unit Models," *IEEE Transactions on Power Apparatus and Systems,* vol. PAS-97, no. 4, pp. 1060-1069, 1978, doi: 10.1109/TPAS.1978.354585.

[9] "Introducing the Phasor Simulation Method." https://uk.mathworks.com/help/physmod/sps/powersys/ug/introducing-the-phasor-simulation-method.html.

[10] "Generic battery model." https://uk.mathworks.com/help/physmod/sps/powersys/ref/battery.html.

[11] "Правила и рекомендации по регулированию частоты и перетоков." https://www.so-ups.ru/fileadmin/files/company/r-n-tpolitics/frequency/specdocs/sto_standard/Pravila_i_rekomendacii_po_regulirovaniju_chastoty_i_peretokov.pdf.